

## An accurate description of 2+1 flavour QCD in a low-energy EFT

---

Sourendu Gupta,<sup>a,\*</sup> Pritam Sen<sup>b</sup> and Rishi Sharma<sup>c</sup>

<sup>a</sup>*International Center for Theoretical Sciences,  
Tata Institute of Fundamental Research,  
Survey 151 Shivakote, Hesaraghatta Hobli, Bengaluru North 560089, India.*

<sup>b</sup>*School of Physical Sciences, Indian Association for the Cultivation of Science,  
2A and 2B Raja S. C. Mullick Road, Kolkata 700032, India.*

<sup>c</sup>*Department of Theoretical Physics, Tata Institute of Fundamental Research,  
Homi Bhabha Road, Mumbai 400005, India.*

*E-mail: [sgupta@theory.tifr.res.in](mailto:sgupta@theory.tifr.res.in), [spsps3333@iacs.res.in](mailto:spsps3333@iacs.res.in),  
[rishi@theory.tifr.res.in](mailto:rishi@theory.tifr.res.in)*

We build an EFT which accurately captures low energy physics of the chiral sector of QCD. When fitted to properties of pions at finite temperature obtained from lattice simulations of 2+1 flavour QCD, it accurately reproduces the crossover temperature seen in the simulations. Its predictions for other quantities are shown. The EFT can then be used for analytic continuation to real time. An interesting property of the continuation is demonstrated.

*The 42nd International Symposium on Lattice Field Theory (LATTICE2025)  
2-8 November 2025  
Tata Institute of Fundamental Research, Mumbai, India*

---

\*Speaker

## 1. The EFT

Chiral symmetry controls many aspects of QCD, including its phase structure. In hadron physics an EFT based on it, namely chiral perturbation theory ( $\chi$ PT) has been immensely successful [1, 2]. Finite size scaling based on it is used to extract a variety of physical quantities [3, 4]. At finite temperature, the NJL model has been used in the past as a toy model of the phase diagram. In [5] we promoted this to a thermal EFT for  $N_f = 2$  by including all terms up to  $D = 6$  allowed by the symmetries. Like all EFTs, this is valid only below some (fairly arbitrary) UV cutoff  $\Lambda$ . In a thermal EFT, Lorentz symmetry is broken to spatial rotations and C, P and T. In addition, the global chiral  $U_B(1) \times SU_L(2) \times SU_R(2)$  symmetry was utilized.

This thermal NJL-like EFT (NJL-TEFT) was dealt with in the Hartree-Fock (HF) approximation to obtain the phase structure. It was further reduced to a thermal  $\chi$ PT (a  $T\chi$ PT), by integrating out all Fermion fluctuations other than the pseudo-Goldstone Bosons (pGBs). This was matched to lattice measurements of low-energy pion properties such as its screening mass,  $m_\pi^D$ , and “velocity”  $u_\pi$ , and the LECs of the NJL-TEFT were extracted from this matching. The EFT then provides a method for Wick-rotating lattice measurements to Minkowski [6]. Note that a computation of  $u_\pi$  in  $\chi$ PT using NLO terms to two-loop order [7] is not compatible with the lattice. This would indicate that any attempt to derive  $T\chi$ PT from  $\chi$ PT requires higher orders.

Here we extend this to  $N_f = 3$ . The generators of  $SU(3)$  are denoted by  $T^a$  with  $1 \leq a \leq 8$ , and we choose to use the representation by Gell-Mann matrices. We also use the notation  $T^0 = (\sqrt{2/3})\mathbb{I}$  for the generator of the remaining  $U(1)$  part of  $U(3)$ . The number of components of the spinors is  $\mathcal{N} = 4N_f N_c$ , since we carry along the colour components for the purposes of  $N_c$  counting. However, there is no global colour symmetry, so only trivial colour transformations are allowed on the spinors, and hence on all composite operators made out of them. There are two issues one has to deal with in extending the EFT to three flavours. The first is that the corresponding EFT with global chiral flavour symmetry up to  $D = 6$  has an accidental  $U_A(1)$  symmetry. This is famously broken only by  $D = 9$  terms. As a result, the theory must include all terms with  $D \leq 9$ , leading to an apparent proliferation of terms. The second issue is that the flavour symmetry is broken in QCD to  $N_f = 2 + 1$ . Since this symmetry breaking is already visible in the deep UV, in the IR the breaking of the symmetry cascades to all operators. It may not be sufficient to break the symmetry only by the mass term. In order to allow for this, we introduce the flavour projection operators,  $\Pi_\ell$  and  $\Pi_s$ , which project fields on to the light and strange quark sectors—

$$\psi_\ell = \Pi_\ell \psi = \frac{1}{\sqrt{3}} \left( \sqrt{2} T^0 + T^8 \right) \psi, \quad \psi_s = \Pi_s \psi = \frac{1}{\sqrt{3}} \left( \frac{1}{\sqrt{2}} T^0 - T^8 \right) \psi, \quad (1)$$

Since flavour  $SU(3)$  is broken to the flavour  $SU(2)$  generated by  $T^a$  with  $1 \leq a \leq 3$ , the other characteristic classes of the original generators will be denoted by  $T^8$  and  $T^m$  with  $4 \leq m \leq 7$ .

We decompose the EFT Lagrangian into a sum of terms at different  $D$ , so  $L = L_3 + L_4 + L_6^3 + L_6^0 + L_8^5 + L_8^2 + L_8^{11} + L_9$ , where  $L_D^N$  denotes terms of dimension  $D$  with  $N$  derivatives. The difference between  $L_8^2$  and  $L_8^{11}$  will be explained later. Terms with  $D = 5$  and  $D = 7$  break either rotational invariance or CPT.  $L_3$  and  $L_4$  are the mass and kinetic terms as usual,

$$L_3 = d_3^\ell \Lambda \bar{\psi}_\ell \psi_\ell + d_3^s \Lambda \bar{\psi}_s \psi_s, \quad \text{and} \quad L_4 = \bar{\psi}_\ell \not{\partial}_4 \psi_\ell + \bar{\psi}_s \not{\partial}_4 \psi_s + d_4^\ell \bar{\psi}_\ell \not{\nabla} \psi_\ell + d_4^s \Lambda \bar{\psi}_s \not{\nabla} \psi_s. \quad (2)$$

These decompositions are obtained since flavour singlet operators can be written in the form  $\Gamma = \Pi_\ell \Gamma \Pi_\ell + \Pi_s \Gamma \Pi_s$ , since the projectors are on to orthogonal subspaces. Similarly one can write

$$L_6^3 = \frac{d_{6,11}^\ell}{\Lambda^2} \bar{\psi}_\ell \nabla^2 \not{\nabla} \psi_\ell + \frac{d_{6,11}^s}{\Lambda^2} \bar{\psi}_s \nabla^2 \not{\nabla} \psi_s. \quad (3)$$

In a vacuum theory, the equation of motion (EoM) up to  $D = 4$  can be used to eliminate any term cubic in derivatives. For EFTs in matter,  $\not{\partial}_4$  and  $\not{\nabla}$  are independent operators, so the EoM can only be used to eliminate one of them. We have chosen to eliminate  $\not{\partial}_4$ .

The decomposition of non-singlet operators uses the fact that  $T^m$  are the only operators which connect the strange and light sectors along with projections of the remaining  $T^i$ 's on the light and strange subspaces. The result is

$$\begin{aligned} L_6^0 = & \frac{d_{6,1}^{\ell\ell}}{\Lambda^2} \left[ (\bar{\psi}_\ell \psi_\ell)^2 + (\bar{\psi}_\ell T^a (i\gamma_5) \psi_\ell)^2 + (\bar{\psi}_\ell (i\gamma_5) \psi_\ell)^2 + (\bar{\psi}_\ell T^a \psi_\ell)^2 \right] + \\ & \frac{d_{6,3}^{\ell\ell}}{\Lambda^2} (\bar{\psi}_\ell \gamma_4 \psi_\ell)^2 + \frac{d_{6,4}^{\ell\ell}}{\Lambda^2} (\bar{\psi}_\ell (i\gamma_i) \psi_\ell)^2 + \frac{d_{6,5}^{\ell\ell}}{\Lambda^2} (\bar{\psi}_\ell \gamma_4 \gamma_5 \psi_\ell)^2 + \frac{d_{6,6}^{\ell\ell}}{\Lambda^2} (\bar{\psi}_\ell (i\gamma_i \gamma_5) \psi_\ell)^2 + \\ & \frac{d_{6,7}^{\ell\ell}}{\Lambda^2} \left[ (\bar{\psi}_\ell T^a \gamma_4 \psi_\ell)^2 + (\bar{\psi}_\ell T^a \gamma_4 \gamma_5 \psi_\ell)^2 \right] + \frac{d_{6,8}^{\ell\ell}}{\Lambda^2} \left[ (\bar{\psi}_\ell T^a (i\gamma_i) \psi_\ell)^2 + (\bar{\psi}_\ell T^a (i\gamma_i \gamma_5) \psi_\ell)^2 \right] + \\ & \frac{d_{6,9}^{\ell\ell}}{\Lambda^2} \left[ (\bar{\psi}_\ell (iS_{i4}) \psi_\ell)^2 + (\bar{\psi}_\ell T^a S_{ij} \psi_\ell)^2 + (\bar{\psi}_\ell T^a (iS_{i4}) \psi_\ell)^2 + (\bar{\psi}_\ell S_{ij} \psi_\ell)^2 \right] + \\ & \frac{d_{6,1}^{ss}}{\Lambda^2} \left[ (\bar{\psi}_s \psi_s)^2 + (\bar{\psi}_s (i\gamma_5) \psi_s)^2 \right] + \frac{d_{6,3}^{ss}}{\Lambda^2} (\bar{\psi}_s \gamma_4 \psi_s)^2 + \frac{d_{6,4}^{ss}}{\Lambda^2} (\bar{\psi}_s (i\gamma_i) \psi_s)^2 + \\ & \frac{d_{6,5}^{ss}}{\Lambda^2} (\bar{\psi}_s \gamma_4 \gamma_5 \psi_s)^2 + \frac{d_{6,6}^{ss}}{\Lambda^2} (\bar{\psi}_s (i\gamma_i \gamma_5) \psi_s)^2 + \frac{d_{6,9}^{ss}}{\Lambda^2} \left[ (\bar{\psi}_s (iS_{i4}) \psi_s)^2 + (\bar{\psi}_s S_{ij} \psi_s)^2 \right] + \\ & \frac{d_{6,1}^{s\ell}}{\Lambda^2} \left[ (\bar{\psi}_s T^m (i\gamma_5) \psi_\ell) (\bar{\psi}_\ell T^m (i\gamma_5) \psi_s) + (\bar{\psi}_s T^m \psi_\ell) (\bar{\psi}_\ell T^m \psi_s) \right] + \\ & \frac{d_{6,3}^{s\ell}}{\Lambda^2} (\bar{\psi}_s \gamma_4 \psi_s) (\bar{\psi}_\ell \gamma_4 \psi_\ell) + \frac{d_{6,4}^{s\ell}}{\Lambda^2} (\bar{\psi}_s (i\gamma_i) \psi_s) (\bar{\psi}_\ell (i\gamma_i) \psi_\ell) + \\ & \frac{d_{6,5}^{s\ell}}{\Lambda^2} (\bar{\psi}_s \gamma_4 \gamma_5 \psi_s) (\bar{\psi}_\ell \gamma_4 \gamma_5 \psi_\ell) + \frac{d_{6,6}^{s\ell}}{\Lambda^2} (\bar{\psi}_s (i\gamma_i \gamma_5) \psi_s) (\bar{\psi}_\ell (i\gamma_i \gamma_5) \psi_\ell) + \\ & \frac{d_{6,7}^{s\ell}}{\Lambda^2} \left[ (\bar{\psi}_s T^m \gamma_4 \psi_\ell) (\bar{\psi}_\ell T^m \gamma_4 \psi_s) + (\bar{\psi}_s T^m \gamma_4 \gamma_5 \psi_\ell) (\bar{\psi}_\ell T^m \gamma_4 \gamma_5 \psi_s) \right] + \\ & \frac{d_{6,8}^{s\ell}}{\Lambda^2} \left[ (\bar{\psi}_s T^m (i\gamma_i) \psi_\ell) (\bar{\psi}_\ell T^m (i\gamma_i) \psi_s) + \bar{\psi}_s T^m (i\gamma_i \gamma_5) \psi_\ell (\bar{\psi}_\ell T^m (i\gamma_i \gamma_5) \psi_s) \right] + \\ & \frac{d_{6,9}^{s\ell}}{\Lambda^2} \left[ (\bar{\psi}_s T^m S_{ij} \psi_\ell) (\bar{\psi}_\ell T^m S_{ij} \psi_s) + (\bar{\psi}_s T^m (iS_{i4}) \psi_\ell) (\bar{\psi}_\ell T^m (iS_{i4}) \psi_s) \right]. \quad (4) \end{aligned}$$

At  $D = 8$  one finds

$$L_8^5 = \frac{d_{8,0}^\ell}{\Lambda^2} \bar{\psi}_\ell \nabla^4 \not{\nabla} \psi_\ell + \frac{d_{8,0}^s}{\Lambda^2} \bar{\psi}_s \nabla^4 \not{\nabla} \psi_s. \quad (5)$$

Other terms with  $D = 8$  contain four fermion fields (two fermion currents) and two derivative operators. The two derivatives can both appear inside one of the currents or one one each of the

two currents. The former we designate as  $L_8^2$  and the latter as  $L_8^{11}$ . An example of the former is  $\bar{\psi}\psi\bar{\psi}\nabla^2\psi$ , and of the latter is  $\bar{\psi}\partial_i\psi\bar{\psi}\partial_i\psi$ . We do not write these out in detail here, since they are too long.

There are only two possible  $D = 9$  terms. These are

$$L_9 = \epsilon_{ff'f''}\epsilon_{gg'g''}(\bar{\psi}^f P_R \psi^g) \left[ \frac{d_{9,1}}{\Lambda^5} (\bar{\psi}^{f'} P_R \psi^{g'}) (\bar{\psi}^{f''} P_R \psi^{g''}) + \frac{d_{9,2}}{\Lambda^5} (\bar{\psi}^{f'} P_R S_{ij} \psi^{g'}) (\bar{\psi}^{f''} P_R S_{ij} \psi^{g''}) \right] + (L \leftrightarrow R), \quad (6)$$

where  $P_{L,R}$  are the projection operators on left and right handed quarks respectively. The first term was obtained by 't Hooft [8] and the second by Schäfer [9]. No other terms of this order are allowed (see the supplementary material of [10]).

## 2. The Gap Equation and fluctuations

The large number of LECs reduce to a much smaller number of combinations in the HF treatment. In order to set it up we introduce two condensates,  $\Sigma_\ell = \Lambda^3 \sigma_\ell$  and  $\Sigma_s = \Lambda^3 \sigma_s$ . Only two independent linear combinations of LECs arise for  $D = 6$ . These are

$$d_6^\ell = \frac{2}{3} \mathcal{N} d_{6,1}^{\ell\ell} - d_{6,3}^{\ell\ell} + 3d_{6,4}^{\ell\ell} + d_{6,5}^{\ell\ell} - 3d_{6,6}^{\ell\ell}, \quad \text{and} \quad d_6^s = \frac{1}{3} \mathcal{N} d_{6,1}^{ss} - d_{6,3}^{ss} + 3d_{6,4}^{ss} + d_{6,5}^{ss} - 3d_{6,6}^{ss}. \quad (7)$$

In the Hartree approximation only the terms in  $\mathcal{N}$  appear. The remaining terms are subleading in  $1/N_c$  and are Fock corrections. The proof that the cross terms between light and strange quarks do not appear in the HF approximation is given in [10]. The terms from  $L_8^2$  and  $L_8^{11}$  do not contribute in the HF approximation as long as the vacuum is kept translation invariant. Then the HF Lagrangian is

$$L_{HF} = -\frac{1}{3} \mathcal{N} \Lambda^4 \left( 2d_6^\ell \sigma_\ell^2 + d_6^s \sigma_s^2 + 2d_9 \sigma_\ell^2 \sigma_s \right) + m_\ell \bar{\psi}_\ell \psi_\ell + \bar{\psi}_\ell \not{\partial} \psi_\ell + m_s \bar{\psi}_s \psi_s + \bar{\psi}_s \not{\partial} \psi_s \\ + d_4^\ell \bar{\psi}_\ell \not{\nabla} \psi_\ell + d_4^s \bar{\psi}_s \not{\nabla} \psi_s + \frac{d_{6,11}^\ell}{\Lambda^2} \bar{\psi}_\ell \nabla^2 \not{\nabla} \psi_\ell + \frac{d_{6,11}^s}{\Lambda^2} \bar{\psi}_s \nabla^2 \not{\nabla} \psi_s \\ + \frac{d_{8,0}^\ell}{\Lambda^4} \bar{\psi}_\ell \nabla^4 \not{\nabla} \psi_\ell + \frac{d_{8,0}^s}{\Lambda^4} \bar{\psi}_s \nabla^4 \not{\nabla} \psi_s. \quad (8)$$

The two effective masses in  $L_{HF}$  are

$$m_\ell = \left( d_3^\ell + 2d_6^\ell \sigma_\ell + d_9 \sigma_\ell \sigma_s \right) \Lambda, \quad \text{and} \quad m_s = \left( d_3^s + 2d_6^s \sigma_s + d_9 \sigma_\ell \sigma_s \right) \Lambda. \quad (9)$$

Note that the terms in the  $d_{6,11}$ s and  $d_{8,0}$ s are the only ones which differ from the form of the mean-field Lagrangian for the NJL model.

Since  $L_{HF}$  is quadratic, a one-loop computation of the free energy,  $F$ , is exact. Typical momenta are of order  $T$ , so the corrections due to the last four terms in eq. (8) go as  $d_{6,11}^{\ell,s} (T/\Lambda)^2$  and  $d_{8,0}^{\ell,s} (T/\Lambda)^4$ . We treat these terms in a series expansion, since they are small. Once  $F$  is written, the as-yet-unknown condensates are determined by the self consistency equations,  $\Sigma_{\ell,s} = dF/dm_{\ell,s}$ . The second derivative of  $F$  gives the positions of the extrema, and putting the solutions of the gap

equations into them, one can find the phase diagram. In the chiral limit we find that the equation for the critical point,  $T_c$ , is given by a polynomial equation [10]. As a result, the critical line can be obtained analytically, and the curvature coefficients  $\kappa_2$  and  $\kappa_4$  can also be computed. When  $d_{6,11}$  and  $d_{8,0}$  vanish the phase boundary is an ellipse, whose shape is completely defined by  $\kappa_2 = 3/(2\pi^2 N_c^2)$  [5]. If the EFT is to describe QCD, which has a single chiral phase transition, the equation for  $T_c$  must have at most one solution. This puts bounds on  $d_{6,11}$  and  $d_{8,0}$ .

With the solution of the gap equation, one can turn from a HF treatment of the action to investigating the fluctuations around it. The most important mode of fluctuations are those with the lowest action, namely the pGBs. There are 9 of these, corresponding to the generators of the unbroken U(3) flavour group. Introducing the pGB fluctuations and integrating over the Fermions gives the T $\chi$ PT Lagrangian  $L_{pGB}$  [11]. Taken up to the  $D = 4$  terms, this contains all the decay constants, the masses, and their mutual couplings.

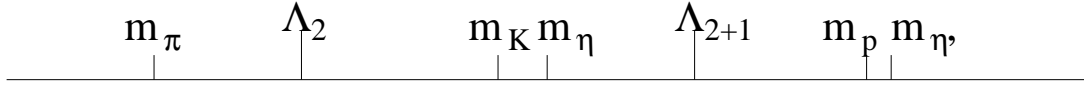


**Figure 1:** Particle masses and UV cutoffs for chiral EFTs. The cutoff for  $N_f = 2$  EFTs should exclude the K meson, so  $\Lambda_2$  must lie between  $m_\pi$  and  $m_K$ . The cutoff for  $N_f = 2 + 1$  has to exclude the proton, so  $\Lambda_{2+1}$  must lie between  $m_\eta$  and  $m_p$ .

Before proceeding further it is useful to consider the UV cutoff of the EFT in more detail. The UV cutoff in a chiral EFT for  $N_f = 2$ , namely  $\Lambda_2$ , should be such that it is able to describe the pions but exclude all strange particles. So one has  $m_\pi < \Lambda_2 < m_K$ . The cutoff of the corresponding EFT with  $N_f = 2 + 1$ , namely  $\Lambda_{2+1}$ , should be able to describe the pseudoscalar meson octet but has to exclude the proton. So one has  $m_\eta < \Lambda_{2+1} < m_p$ . This is summarized in Figure 1. It has been shown that vector mesons are generated in chiral EFTs when the S-matrix is unitarized [12], so the  $\rho$  meson places no restriction on  $\Lambda_{2+1}$ . Since  $m_{\eta'} > m_p$ , chiral EFTs will be unable to treat the  $\eta'$  meson when the quark masses are tuned to realistic values.

As we expect, in  $L_{pGB}$  the  $\eta'$  mass is split from the remaining pGBs by  $d_9$ . As a result, by tuning this we can push  $m_{\eta'}$  beyond  $\Lambda_{2+1}$  and obtain a theory with only the flavour SU(3) octet of pseudoscalar mesons. In  $L_{pGB}$ , if we integrate over all the modes between  $\Lambda_{2+1}$  and  $\Lambda_2$  we will be left with only the pions. This action,  $L_\pi$ , has the form

$$L_\pi = \frac{1}{2}\Lambda_2^2 c_2 \phi_a^2 + \frac{1}{2}\phi_a^2 + \frac{1}{2}c_4 (\nabla\phi_a)^2 + \frac{1}{8}c_{41}\phi_a^4 + \dots \quad (10)$$

where we show only the terms up to  $D = 4$ . The pion mass is  $m_\pi^2 = c_2\Lambda_2^2$ ,  $u_\pi^2 = c_4$ , and there is an overall normalization of the pion field operator which gives a scale factor  $f^2$ . Of course, we expect chiral power counting to work, and the term in the pion self-coupling  $c_{41}$  should be NLO in this counting. We verified that it is, and that it vanishes in the chiral limit as  $c_2$ . We note that the Debye screening mass of the pion is  $m_\pi^D = m_\pi/u_\pi$  and the pion decay constant  $f_\pi = fu_\pi$ . When these LECs are matched to lattice measurements for  $N_f = 2 + 1$ , then eq. (10) contains the effects of strange mesons even though there are no explicit fields for them.

In [5] we had shown how to start from a NJL-TEFT for  $N_f = 2$  and obtain eq. (10) from it. In other words, we could write the LECs  $c_2$ ,  $c_4$  and  $c_{41}$  in terms of the quark LECs. By sufficient

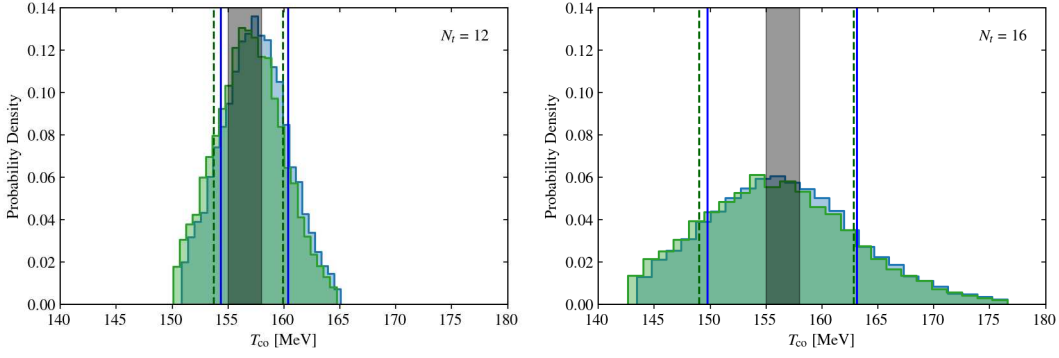


**Figure 2:** Bootstrap histogram (blue for  $d_3 = 0.12$ , green for  $d_3 = 0.125$ ) for the crossover temperature,  $T_{co}$ , predicted by the EFT when it is matched only to pion properties. The vertical lines enclose the 68% CL of  $T_{co}$ , and the vertical gray band is the 68% CL from the direct lattice measurement [15]. Due to the different statistical errors in the measurement of  $m_\pi^D$  on  $N_f = 12$  and 16 lattices, the predicted errors on  $T_{co}$  are different.

number of lattice measurements in  $N_f = 2 + 1$  QCD, one can determine all the quark LECs. This gives an effective  $N_f = 2$  NJL-TEFT in which there are no explicit strange quarks, but their effects are included in the light quark LECs. Then these LECs can be used in any computation one wishes for momenta less than  $\Lambda_2$ .

### 3. Matching to lattice

The  $N_f = 2$  NJL-TEFT in the HF approximation can be easily written down from an examination of eq. (8). One first drops all terms which come from strange quarks. Then one notes that there is no accidental axial U(1) symmetry for  $D = 6$ . Indeed one sees that this accidental symmetry is broken by terms which have  $D = 3N_f$ . For  $N_f = 2$  a simple Fierz rearrangement of the determinant terms can be used to absorb them into  $L_6^0$ . Retaining only terms up to  $D = 6$ , one can simply drop the  $d_{8,0}$  term. Then the number of LECs to be determined is 4, namely  $d_3$ ,  $d_4$ ,  $d_6$  and  $d_{6,11}$ .

Matching to lattice measurements of the curvature of the critical line,  $\kappa_2$ , one finds that  $d_{6,11}$  is vanishing. Of the remaining three LECs,  $d_3$  is seen not to change significantly with temperature, so it is found by matching to pion mass at  $T = 0$ . The two remaining LECs are obtained by matching  $m_\pi^D$  at two different temperatures below the crossover  $T_{co}$ . Errors on the LECs are induced by the errors in the lattice measurements that we match, and these are propagated to the predictions of the EFT. We used a bootstrap to find the uncertainties in the EFT predictions which result from matching to quantities with errors. This was implemented by sampling input lattice measurements from Gaussian distributions with the reported means and standard errors. For each sample various EFT predictions were constructed.

We note that  $N_f = 2$  measurements of thermal pion two-point functions were used in [13] to measure both  $m_\pi^D$  and  $u_\pi$ , giving two independent measurements at each temperature. Unfortunately, the  $N_f = 2 + 1$  measurements of [14] only quote screening masses. We hope that the success of this approach (reported in the next section) prompts future lattice measurements of the screening masses,

the velocity parameters, and the thermal decay constants of each member of the pseudoscalar octet. This would allow a full determination of all the LECs which enter eq. (8), with enough left over for testing the EFT.

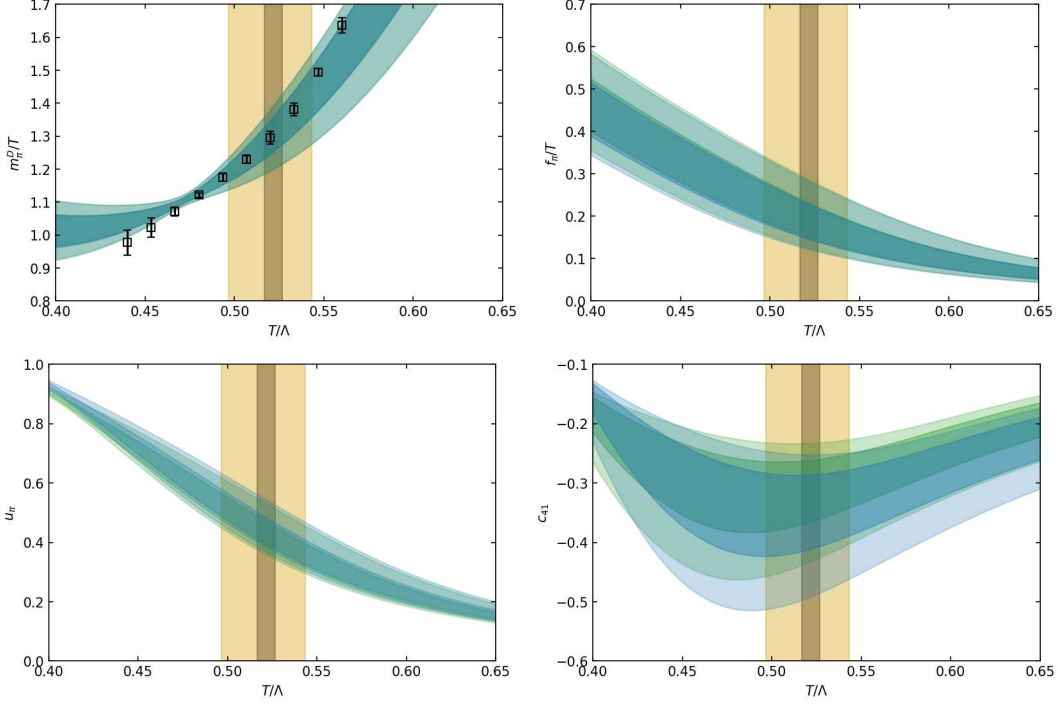


**Figure 3:** Predictions from the EFT with  $\Lambda_2 = 300$  MeV (blue for  $c_3 = 0.12$  and green for  $c_3 = 0.125$ , darkest shade for 68% CL, progressively lighter for 90% and 95%). Vertical bands show the 66% CL for  $T_{co}$  (dark brown for the lattice determination and lighter for the EFT prediction). From top left (moving clockwise) the figures show the temperature dependence of the pion Debye screening mass  $m_\pi^D$ , the thermal pion decay constant  $f_\pi$ , the pion four-point self coupling  $c_{41}$  and the pion velocity  $u_\pi$ . The symbols for  $m_\pi^D$  are the continuum extrapolated lattice determinations of [14].

For both values of  $\Lambda_2$  we matched the LECs to the lattice measurements of [14] for both  $N_t = 12$  and 16. The lattice cutoffs,  $1/a$  (where  $a$  is the lattice spacing), for both are larger than  $\Lambda_2$ . So, for the EFT should not be able to resolve the differences between them. This is indeed so, and the EFT gives the same predictions from both sets of inputs (for example see Figure 2).

Since the UV cutoff is a pseudo-parameter, we performed two matches, one with  $\Lambda_2 = 300$  MeV and another with  $\Lambda_2 = 450$  MeV. With the same input data the values of the LECs are different of course, however the EFT predictions of  $T_{co}$  and the critical temperature in the chiral limit,  $T_c$ , are equal within errors, and in agreement with lattice determinations.

#### 4. Results

We explained in the previous section that apart from  $d_{6,11}$ , the other LECs are all matched to pion properties. This is a deliberate choice, since the prediction of the EFT for  $T_{co}$  and the critical temperature in the chiral limit,  $T_c$ , are then a test of the universality argument underlying

this approach. Figure 2 shows the bootstrap histogram for the prediction of  $T_{co}$  and a comparison with its lattice determination. There is a good match. The errors in the EFT prediction would decrease if the accuracy of pion measurements were to be improved.

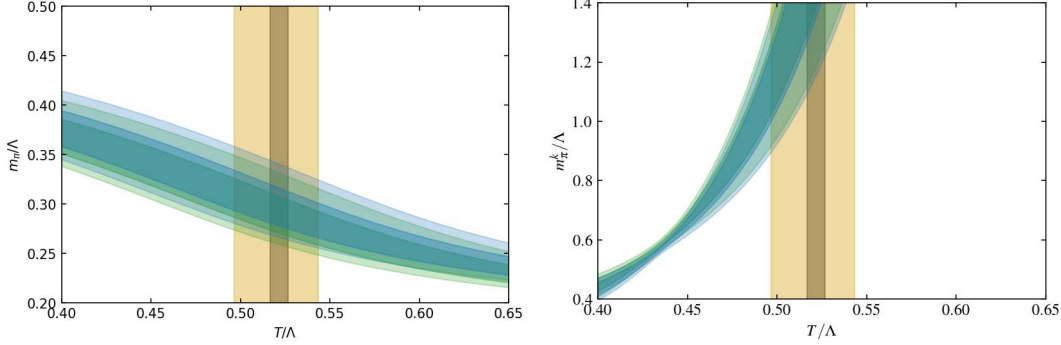


**Figure 4:** Predicted pion pole mass  $m_\pi$  (left) and pion kinetic mass  $m_\pi^k$  (right) from the EFT with  $\Lambda_2 = 300$  MeV (blue for  $c_3 = 0.12$  and green for  $c_3 = 0.125$ , darkest shade for 68% CL, progressively lighter for 90% and 95%). Vertical bands show the 66% CL for  $T_{co}$  (dark brown for the lattice determination and lighter for the EFT prediction).

In Figure 3 we show the predictions of the EFT for various pion properties. As discussed earlier, two values of  $m_\pi^D$  for  $N_t = 16$  [14] were used for matching. The continuum results were not inputs. Note that  $m_\pi^D$ ,  $u_\pi$  and  $f_\pi$  can all be obtained from 2-point functions of pions and the axial current. The self-coupling  $c_{41}$  can be obtained from measurements of 4-point functions of pions. As a result, these predictions can easily be checked on the lattice. Note the continuity of the results across  $T_{co}$ , and the agreement of  $m_\pi^D$  above  $T_{co}$  with the predictions of the EFT. Since this is a crossover, it is not surprising that a hadron description remains viable, at least in the vicinity of  $T_{co}$ .

When  $L_\pi$  is written in the Lorentz metric, then the dispersion relations are [6]

$$E(p) = \sqrt{m_\pi^2 + u_\pi^2 p^2} \simeq m_\pi + \frac{1}{2} \frac{p^2}{m_\pi^k} + O(p^4), \quad (11)$$

where the mass parameter in the kinetic energy term (for small momenta,  $p$ ) contains the kinetic mass  $m_\pi^k = m_\pi/u_\pi^2$ . In the limit of vanishing  $p$ , the particle energy is its rest mass,  $m_\pi$ . This has also been called the pole mass in the lattice literature. In Figure 4 we show  $m_\pi$  and  $m_\pi^k$  predicted in the EFT. Note that when  $T/T_{co} = 0.77$  then the pion rest mass is predicted to drop to the range 105–120 MeV. At  $T_c$  we find  $m_\pi \simeq 90$  MeV.

The increase of  $m_\pi^k$  shown here indicates that the kinetic energy rises slower with  $p$  than might be expected from a consideration of the rest mass. Also this becomes even slower as the temperature increases. This indicates that reaction channels which were available at  $T = 0$  quickly switch off as the temperature increases. Also, since  $m_\pi^k$  is of the order of  $\Lambda_2$  at  $T_{co}$ , real time physics can not be done with  $L_\pi$  at this point, and NJL-TEFT must be used. It is interesting that this EFT shows a continuity of the hadron description above  $T_{co}$  in imaginary time Euclidean and its breakdown in Minkowski real time.

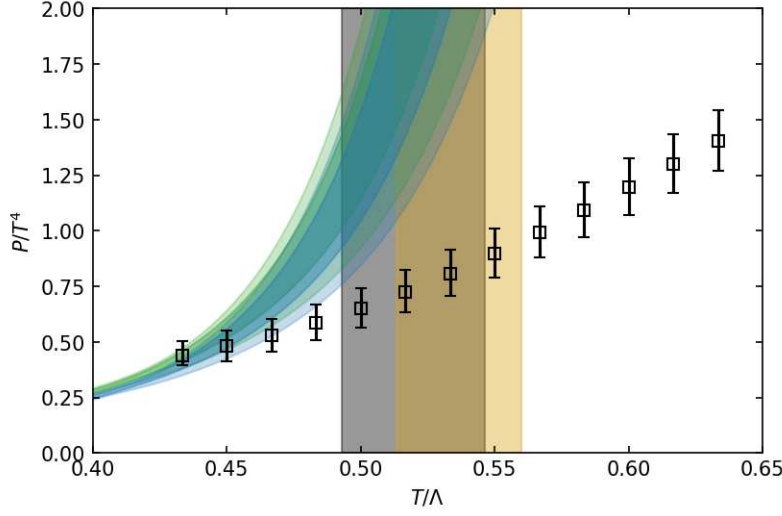


**Figure 5:** The bands show the EFT (with  $\Lambda = 300$  MeV) predictions for the pressure  $P$  of QCD with  $N_f = 2 + 1$  at finite temperature  $T$  (darkest for 68% CL, lighter for 90% and lightest for 95%, in blue for  $d_3 = 0.12$  and green for  $d_3 = 0.125$ ). Symbols and error bars show the lattice measurements. Vertical bands (blue and green) show the EFT predictions for  $T_{co}$  and the brown band of the lattice.

When the UV cutoff,  $\Lambda$ , of the EFT is sufficiently higher than the temperature  $T$ , then it may be possible to understand the equation of state (EoS) of matter. We investigated the pressure,  $P$ , with the results shown in Figure 5. It is surprising that the predictions of the EFT are anywhere close to the lattice measurements, given the neglect of gluon modes. Whether the remaining mismatch is due to the neglect of NLO terms in the EFT or to the missing gluons remains a matter for future investigation.

## References

- [1] J. Gasser and H. Leutwyler, *Annals Phys.* **158**, 142 (1984)
- [2] J. Gasser and H. Leutwyler, *Nucl. Phys. B* **250**, 465-516 (1985)
- [3] O. Kaczmarek, F. Karsch, A. Lahiri, S. T. Li, M. Sarkar, C. Schmidt and P. Scior, *PoS LATTICE2021*, 429 (2022) [arXiv:2112.15398 [hep-lat]].
- [4] D. A. Clarke, P. Dimopoulos, F. Di Renzo, J. Goswami, C. Schmidt, S. Singh and K. Zambello, *PoS LATTICE2023*, 168 (2024) doi:10.22323/1.453.0168 [arXiv:2401.08820 [hep-lat]].
- [5] S. Gupta and R. Sharma, *Phys. Rev. D* **97**, no. 3, 036025 (2018) [arXiv:1710.05345 [hep-ph]].
- [6] S. Gupta and R. Sharma, *Int. J. Mod. Phys. A* **35**, no.33, 2030021 (2020) [arXiv:2006.16626 [hep-ph]].
- [7] D. Toublan, *Phys. Rev. D* **56**, 5629-5645 (1997) doi:10.1103/PhysRevD.56.5629 [arXiv:hep-ph/9706273 [hep-ph]]

- [8] G. 't Hooft, Phys. Rept. **142**, 357-387 (1986)
- [9] T. Schäfer, Phys. Rev. D **65**, 094033 (2002) [arXiv:hep-ph/0201189 [hep-ph]].
- [10] S. Gupta, P. Sen and R. Sharma, [arXiv:2511.00409 [hep-lat]].
- [11] S. Weinberg, “The Quantum Theory of Fields: Volume 2, Modern Applications”, Cambridge University Press, Cambridge, 1996.
- [12] A. Gomez Nicola and J. R. Pelaez, Phys. Rev. D **65**, 054009 (2002) [hep-ph/0109056].
- [13] B. B. Brandt, A. Francis, H. B. Meyer and D. Robaina, Phys. Rev. D **90** (2014) no.5, 054509 [arXiv:1406.5602 [hep-lat]].
- [14] A. Bazavov, S. Dentinger, H. T. Ding, P. Hegde, O. Kaczmarek, F. Karsch, E. Laermann, A. Lahiri, S. Mukherjee and H. Ohno, *et al.* Phys. Rev. D **100**, no.9, 094510 (2019) [arXiv:1908.09552 [hep-lat]].
- [15] A. Bazavov *et al.* [HotQCD], Phys. Lett. B **795** (2019), 15-21 [arXiv:1812.08235 [hep-lat]].